

September 11, 1998

---

# Study of the TT2/TT10 Transfer Line Optics via Transfer Matrix Measurement

G. Arduini, M. Giovannozzi, K. Hanke,  
J.-Y. Hémerly

Keywords: SPS Machine, Optics

Run no.	Date
	03/07/98

---

---

## Summary

A good matching between the optics parameters at the extraction point in the PS ring and those at the injection point in the SPS ring must be performed in order to minimize the emittance blow-up of the beams at injection. The TT2/TT10 transfer line optics was modelled and matched using the program package *MAD*. The model relies on a good knowledge of the calibration curves for the quadrupoles and might be hampered by hardware errors e.g. inter-turn coil shorts. In order to verify the calibration curves and test the absence of hardware faults, the sine-like component of the transfer matrix has been measured deflecting the beam by means of dipole correctors. The results of the measurement were found in good agreement with those obtained from the *MAD* model.

---

## 1 Introduction

The beam optics of the TT2/TT10 transfer line is presently subject to intense studies. As a part of the LHC injection chain, an emittance blow-up of no more than 5% is allowed in the transfer from the PS to the SPS in order to meet the luminosity requirements. Furthermore, good matching of the transfer line is required for the large-emittance fixed target beams to minimize beam losses and therefore radiation. These requirements can only be fulfilled provided the optics of the transfer line is well understood. As a first step, a *MAD* [1] model of the complete TT2/TT10 line was created [2]. While the geometry of the beam line was cross checked versus the CERN survey data, the magnetic behaviour of the elements can only be tested by measuring selected elements of the transfer matrix. This can be achieved by deflecting the beam using well defined kicks, generated by the trajectory correctors, and observing whether its behaviour is correctly described by the model. This procedure allows in particular to identify faults in the transfer line hardware, e.g. quadrupole shorts, wrong scaling factors in the power supplies etc.

## 2 Measurement Technique

The standard approach to measure the sine-like component of the transfer matrix of a beam line consists in exciting transverse betatron oscillations. Dipole magnets are used to deflect the beam and the resulting trajectory is then measured on a set of monitors. If  $\mathcal{M}_{i,j}$  stands for the transfer matrix between the  $i$ th

corrector and the  $j$ th monitor, and we assume that no linear coupling is present, the beam position at the monitor location is given by

$$x_i = (\mathcal{M}_{i,j})_{1,2} \vartheta_H, \quad y_i = (\mathcal{M}_{i,j})_{3,4} \vartheta_V,$$

where  $x_i, y_i$  represents the horizontal and vertical position on monitor  $i$  and  $\vartheta$  is the deflection angle produced in one of the planes. The unknown matrix element can be computed by simply varying the deflection angle: the slope of the straight line representing the beam position as a function of the angle is the required quantity.

### 3 Experimental Results

In the TT2 line five bending dipoles are installed which are normally used to steer the beam. Three of them are horizontal correctors (BHZ117, BHZ147, BHZ167) and two are vertical deflectors (BVT123, BVT173).

The five elements were varied one at a time, and for each element three settings were applied. The deflection angle can be deduced from the current using the corresponding conversion factors.<sup>1</sup> The three settings have been determined in order to have the maximum excursion in the deflection angle and beam position, while remaining in the transfer line acceptance. Table 1 shows settings and conversion factors for the five dipole correctors used to deflect the beam.

element	setting 1 [A]	setting 2 [A]	setting 3 [A]	conv. factor [mrad/A]	$\mu_H$ [2 $\pi$ ]	$\mu_V$ [2 $\pi$ ]
BHZ117	179.07	184.07	174.07	6.17 / B $\rho$	7.03450	13.8626
BHZ147	202.67	205.67	200.67	6.17 / B $\rho$	11.6595	13.8929
BHZ167	156.82	160.82	153.00	- 4.87 / B $\rho$	19.5715	13.9454
BVT123	275.80	280.80	271.80	5.59 / B $\rho$	40.9064	14.0053
BVT173	274.18	278.18	271.18	- 5.59 / B $\rho$	44.2594	14.0212

Table 1: Element settings, conversion factors and phase advance for the five dipole correctors used to deflect the beam.

The betatron phase at the location of the five elements was determined using the *MAD* model [2]. The numerical values are given in Tab. 1. In each plane, at least two correctors are separated by a phase advance which is an odd multiple of  $90^\circ$  thus allowing a complete test of the transfer line optics.

Using the secondary emission monitors (SEM-fils) in TT2 as well as SEM-grids, optical transition radiation (OTR) monitors and couplers in TT10, the beam position could be recorded at 16 different locations along the transfer line. For each monitor, a linear fit through the three values yields the change of beam position per unit deflection angle, i.e. the matrix element  $(\mathcal{M}_{i,j})_{1,2}$  or  $(\mathcal{M}_{i,j})_{3,4}$ . This procedure was repeated for all the five bending dipoles. The results for the horizontal plane are shown in Figs. 1 - 3. The horizontal axis shows the position of the beam monitors in the transfer line. On the vertical axis, the matrix element is plotted. The circles represent the measured data. The corresponding plots for the vertical plane are shown in Figs. 4 and 5.

<sup>1</sup>To follow the same convention as used by *MAD*, the sign must be inverted in some cases.

## 4 MAD Simulation

The *MAD* model of the TT2/TT10 line was used to simulate the optics for the 26 GeV/c beam during the measurement. Zero-length kicker elements were placed at the exit of the bending magnets used in the experiment, and their deflection angle was set to 1 mrad. The change of beam position with respect to the original setting was saved at all the monitor locations. The values are plotted as stars in Figs. 1 - 5. In general, there is a rather good agreement between experimental data and the simulation results. The remaining discrepancy between model and measurement can be explained by constant factors. In Fig. 6 the measured data are plotted versus the *MAD* results. The dependence is linear for all five dipoles. The factors obtained from linear fits shown by the solid lines are given in Tab. 2.

element	slope	error
BHZ117	0.7565	0.0021
BHZ147	0.8014	0.0046
BHZ167	0.6712	0.0056
BVT123	0.6729	$1 \times 10^{-5}$
BVT173	0.8198	$1 \times 10^{-5}$

Table 2: Factors found between measured values and *MAD* values.

Figures 7 - 11 show *MAD* values and experimental data, while the measured values have now been corrected with the factors obtained. The agreement is now within the error. Taking into account the phase advance of the correctors we exclude the possibility of a faulty element.

## 5 Conclusion

The good agreement of the real behaviour of the beam and the *MAD* simulation proves the validity of the model. While the geometry of the model had already been cross-checked versus the survey data [2], now also the correct magnetic behaviour of the elements could be verified. From the results of the measurements presented in this note, one can exclude the event of a magnetic fault in one of the elements of the transfer line.

## Acknowledgements

We would like to thank the operation crew for the support during the experimental session. Many thanks to D. Manglunki, M. Martini and G. Métral for setting up the fast extracted beam and for discussions.

## References

- [1] H. Grote, F. C. Iselin, *The MAD Program, User's Reference Manual*, CERN SL (AP) 90-13 (1990).
- [2] G. Arduini, M. Giovannozzi, K. Hanke, J-Y. Hémerly, M. Martini, *MAD and BeamOptics Description of the TT2/TT10 Transfer Lines*, CERN SL (OP) 98-040 and CERN PS (CA) 98-014 (1998).

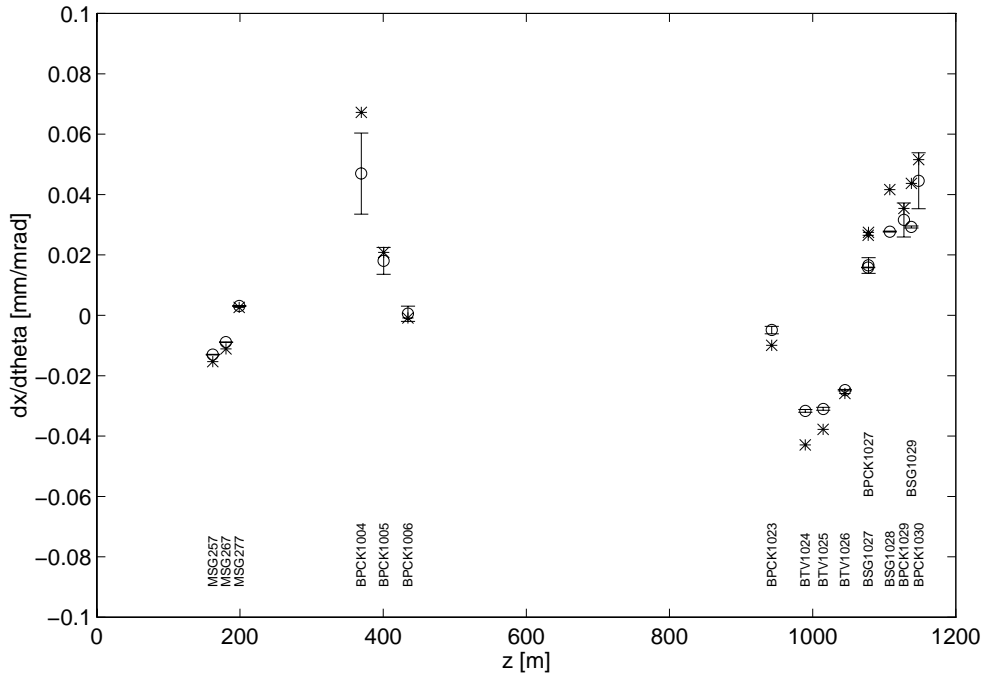


Figure 1: Change of beam position in [mm/mrad] for horizontal kicks generated using the BHZ117 bending dipole. The circles represent the measured values, the stars correspond to the MAD model.

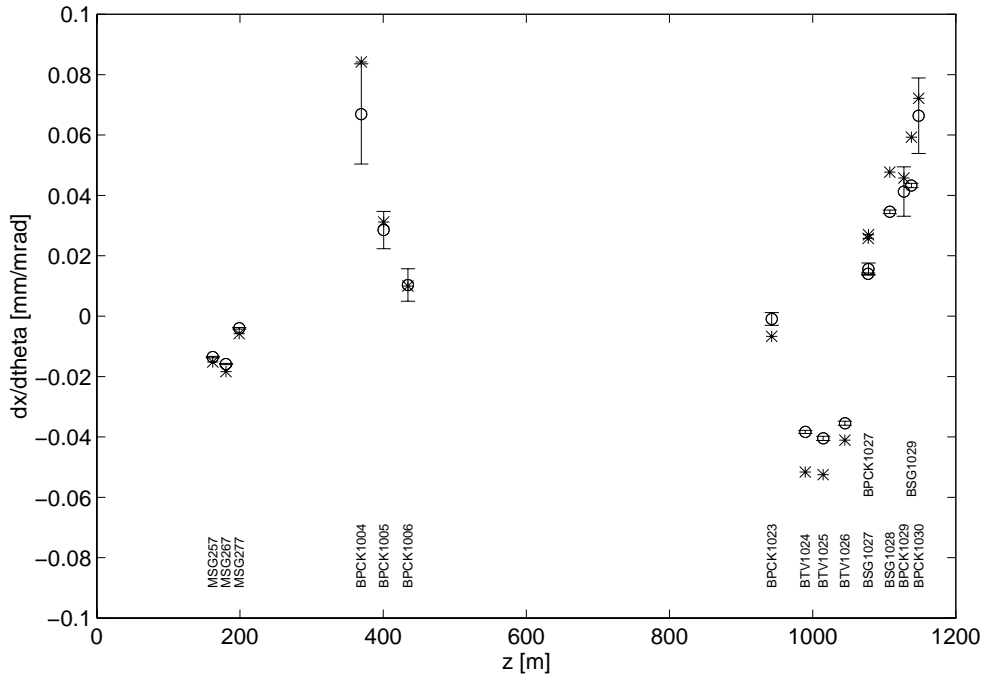


Figure 2: Change of beam position in [mm/mrad] for horizontal kicks generated using the BHZ147 bending dipole. The circles represent the measured values, the stars correspond to the MAD model.

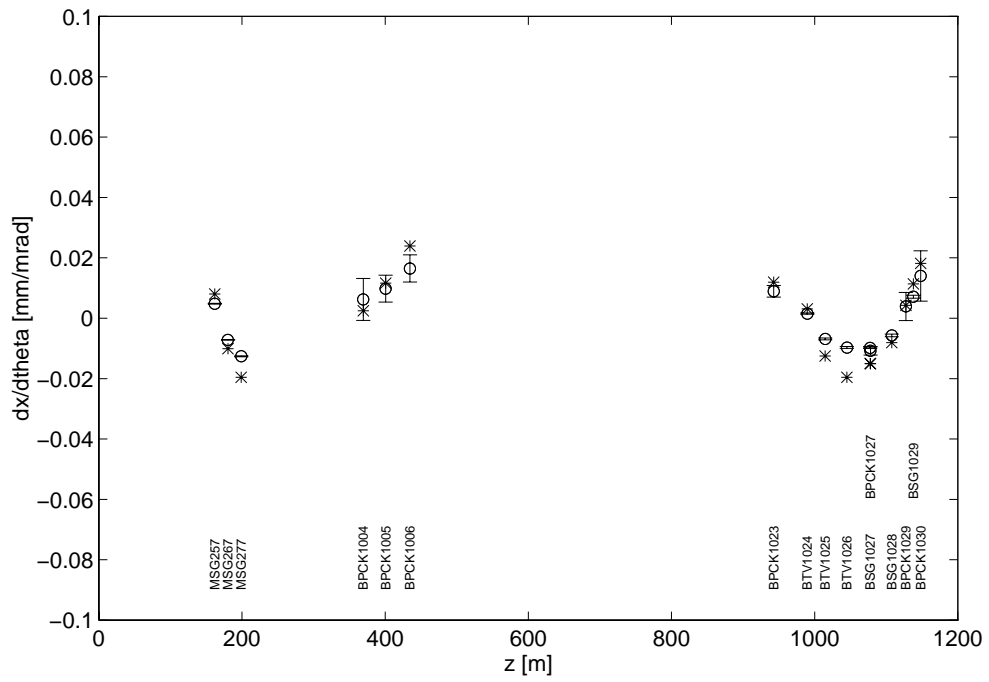


Figure 3: Change of beam position in [mm/mrad] for horizontal kicks generated using the BHZ167 bending dipole. The circles represent the measured values, the stars correspond to the MAD model.

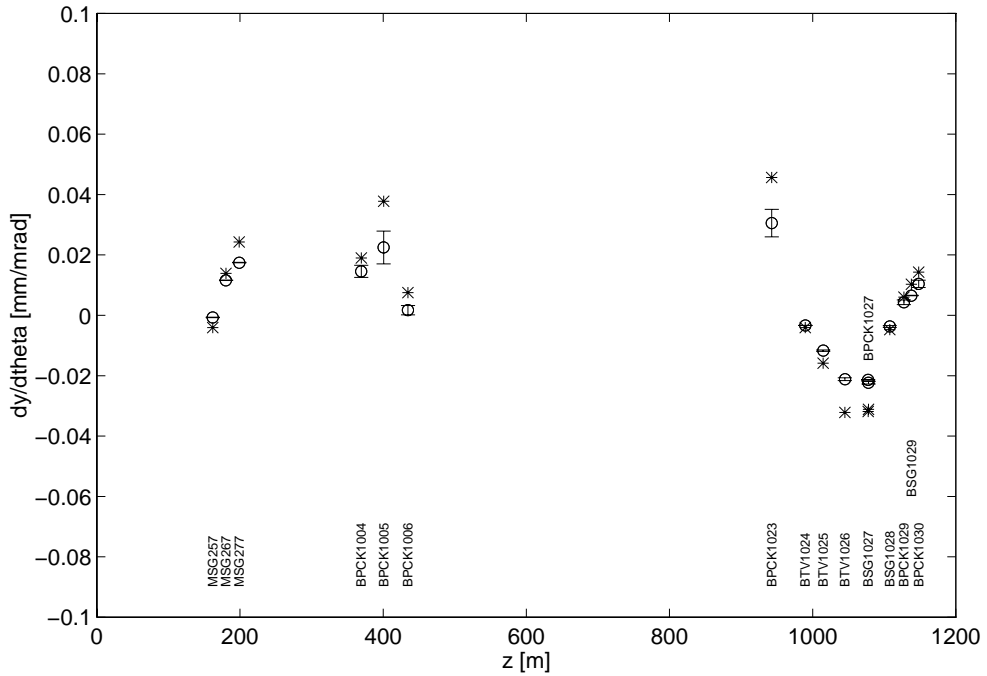


Figure 4: Change of beam position in [mm/mrad] for vertical kicks generated using the BVT123 bending dipole. The circles represent the measured values, the stars correspond to the MAD model.

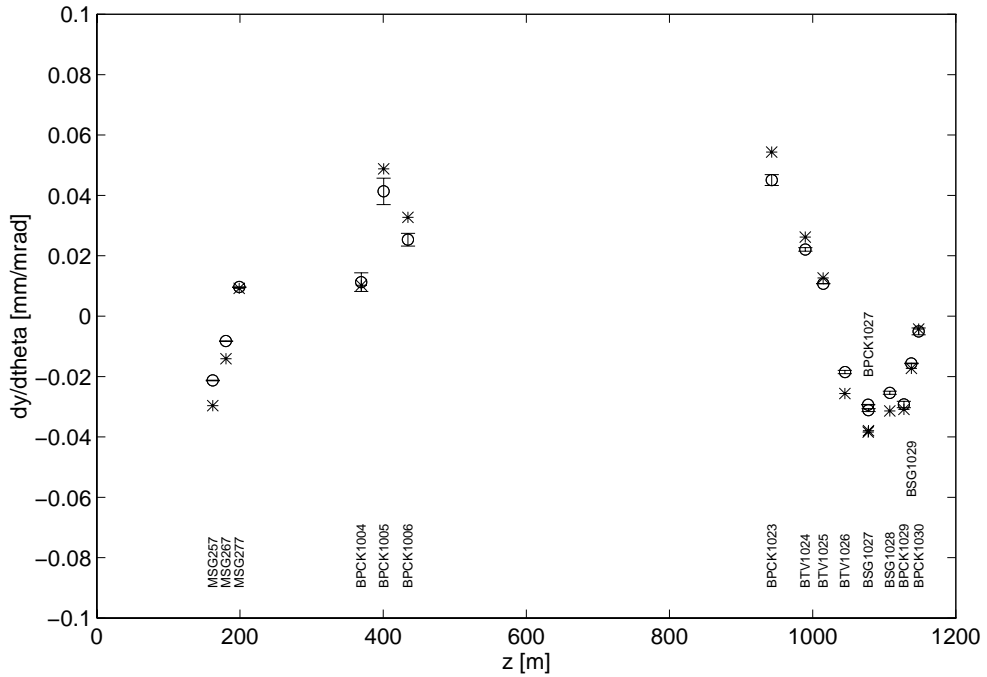


Figure 5: Change of beam position in [mm/mrad] for vertical kicks generated using the BVT173 bending dipole. The circles represent the measured values, the stars correspond to the MAD model.

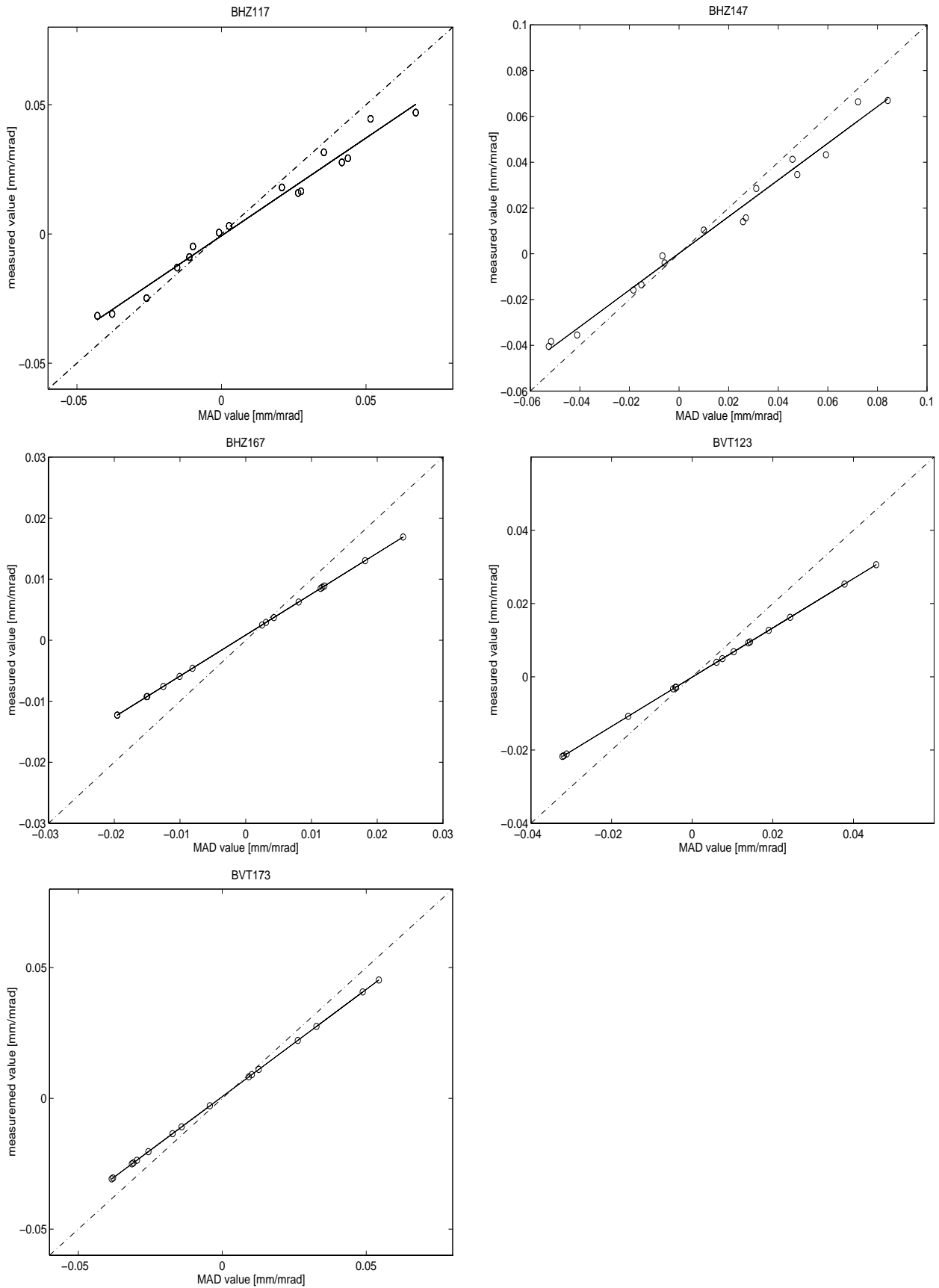


Figure 6: Measured values versus *MAD* values for the five elements used for the measurement.



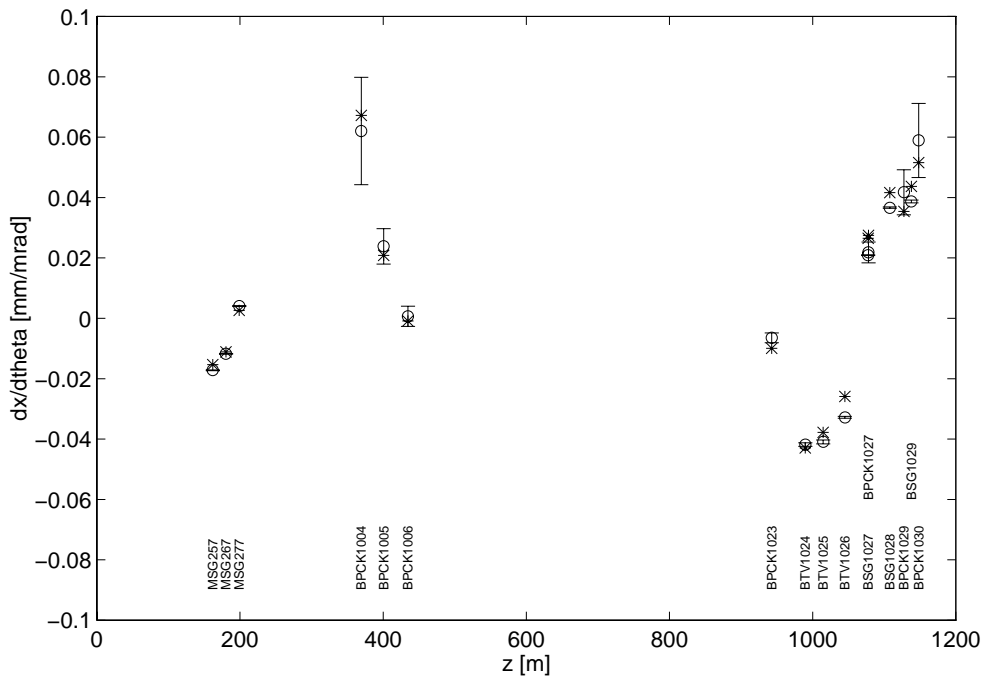


Figure 7: Change of beam position in [mm/mrad] for horizontal kicks generated using the BHZ117 bending dipole. The circles represent the corrected experimental data, the stars correspond to the MAD model.

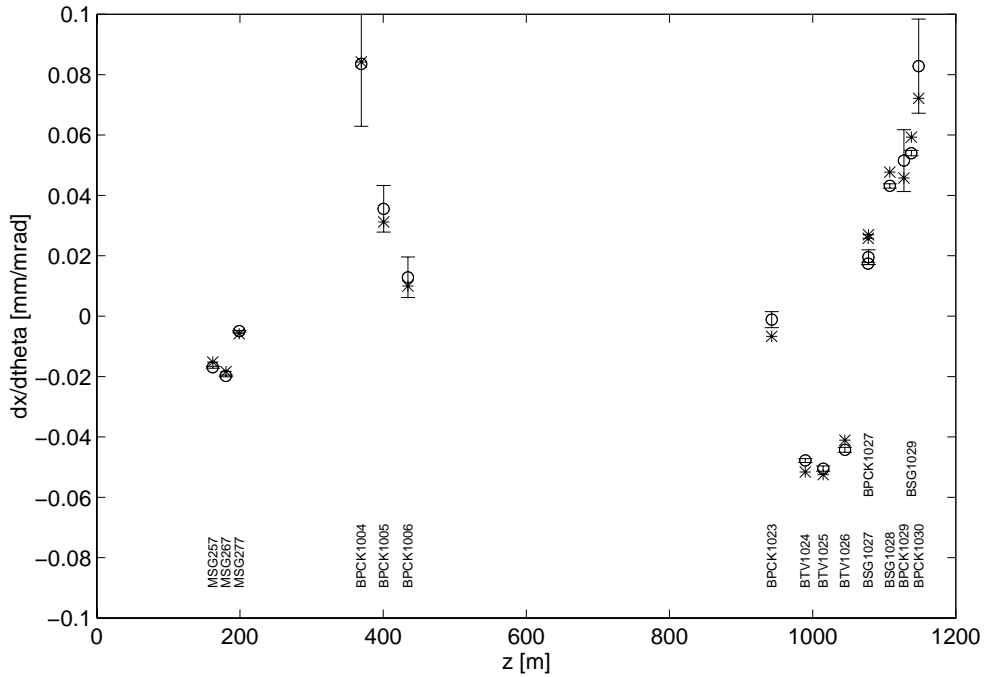


Figure 8: Change of beam position in [mm/mrad] for horizontal kicks generated using the BHZ147 bending dipole. The circles represent the corrected experimental data, the stars correspond to the MAD model.

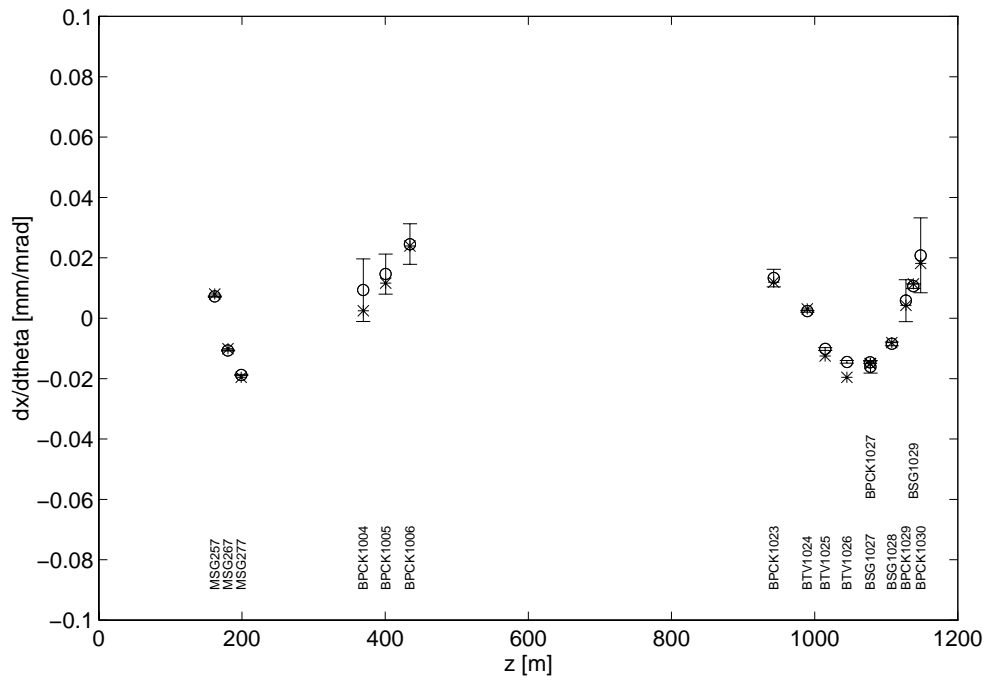


Figure 9: Change of beam position in [mm/mrad] for horizontal kicks generated using the BHZ167 bending dipole. The circles represent the corrected experimental data, the stars correspond to the MAD model.

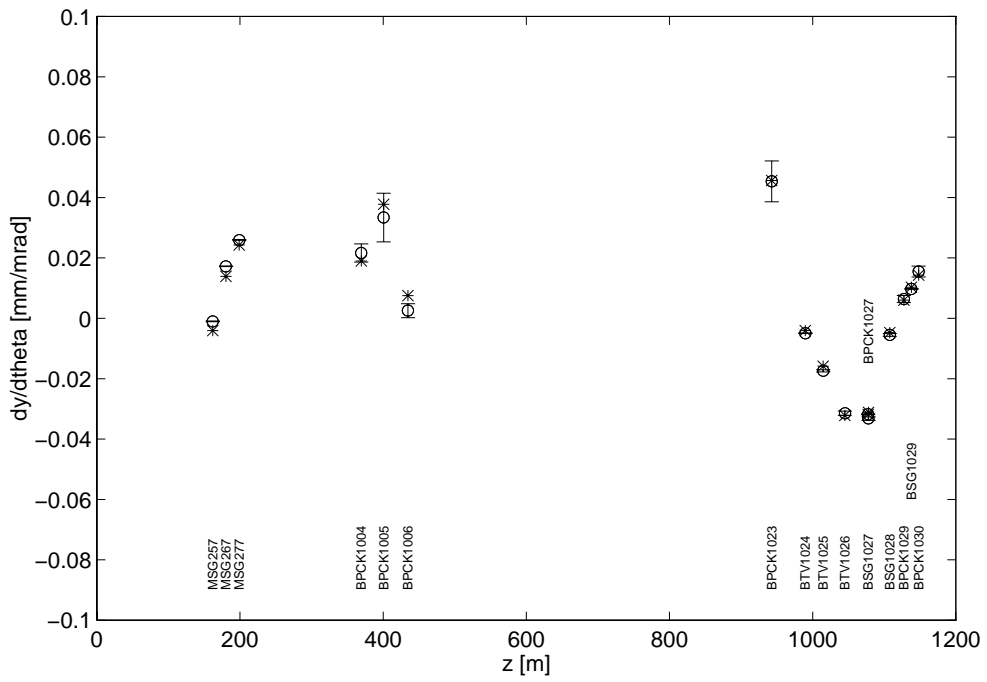


Figure 10: Change of beam position in [mm/mrad] for vertical kicks generated using the BVT123 bending dipole. The circles represent the corrected experimental data, the stars correspond to the MAD model.

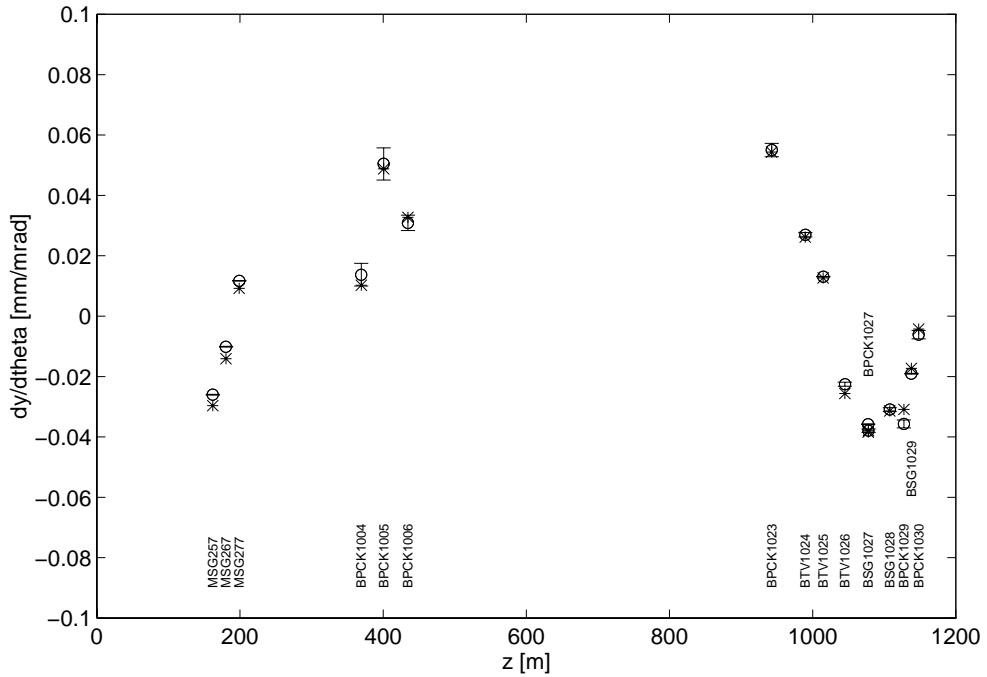


Figure 11: Change of beam position in [mm/mrad] for vertical kicks generated using the BVT173 bending dipole. The circles represent the corrected experimental data, the stars correspond to the MAD model.

# Distribution List

B. Autin	PS/DI
J. Boillot	PS/OP
R. Cappi	PS/CA
M. Giovannozzi	PS/CA
J-Y. Hémary	PS/CA
M. Lindroos	PS/OP
D. Manglunki	PS/CA
M. Martini	PS/CA
G. Métral	PS/OP
J-P. Riunaud	PS/CA
K. Schindl	PS/DI